

Nonthermal Occupation of Higher Subbands in Semiconductor Superlattices via Sequential Resonant Tunneling

H. T. Grahn, H. Schneider,^(a) W. W. Rühle, K. von Klitzing, and K. Ploog

Max-Planck-Institute für Festkörperforschung, Heisenbergstrasse 1,
D-7000 Stuttgart 80, Federal Republic of Germany

(Received 21 November 1989)

We report on the observation of photoluminescence from the second and third electronic subbands in undoped GaAs-AlAs superlattices under application of an electric field perpendicular to the layers. The occupation of the higher subbands is achieved by sequential resonant tunneling of electrons. We determine the relative occupation of the second subband at resonance. Together with the electrically measured transport time between adjacent wells this novel spectroscopic effect provides a new method to determine the intersubband relaxation time.

PACS numbers: 79.80.+w, 72.20.Jv, 72.40.+w, 78.47.+p

The occupation of higher subbands and the lifetime of excited states in semiconductor quantum wells (QW's) and superlattices (SL's) has been the subject of great current interest and of some controversy. In a recent publication¹ it was shown via intersubband emission experiments that higher subbands in GaAs-Al_xGa_{1-x}As superlattices can be occupied by sequential resonant tunneling (SRT). However, this type of experiment was only possible for intersubband transitions with an energy below the optical-phonon energy in GaAs. This suggests that the emission of optical phonons is an important process in the intersubband energy relaxation of carriers in QW's and SL's. The lifetime of electrons in higher subbands in quantum wells has been investigated by a variety of experimental techniques.²⁻⁵ The reported intersubband scattering times vary over more than 1 order of magnitude. Furthermore, intersubband scattering in quantum wells has recently attracted significant theoretical interest.^{6,7} According to a recent calculation⁷ the intersubband scattering time due to slab phonons should depend strongly on the barrier height. It decreases with increasing Al content in Al_xGa_{1-x}As barriers.

In this Letter we report the first observation of band-to-band photoluminescence (PL) from excited subbands in undoped semiconductor superlattices under weak illumination. The occupation of the higher subbands is a result of SRT of electrons in an electric field perpendicular to the layers. The occupation of the second subband exhibits a maximum for resonant coupling of the wells, i.e., when the second and first subbands are aligned in adjacent wells. The ratio of occupation between the second and first subbands obtained from the corresponding PL intensities is used to determine the intersubband scattering time in this system. The energy spacing between the first and second subbands is larger than the optical-phonon energy in GaAs.

The samples are GaAs-AlAs superlattices with fifty periods sandwiched between *p* and *n* layers of Al_{0.5}Ga_{0.5}As in a *p-i-n* structure. The structures are

grown by molecular-beam epitaxy on a (100)-oriented *n*⁺-type GaAs substrate. The superlattices are nominally undoped. The thickness of the GaAs wells is 12.3 nm in sample I and 11.8 nm in sample II with respective AlAs barriers of 2.1 and 1.6 nm. The *p-i-n* diodes are processed into mesas of 0.004 mm² area with Ohmic Cr/Au contacts on both sides.

Electrical time-of-flight experiments demonstrate that SRT contributes to the transport in superlattices. Furthermore, the transport times through the whole superlattice are obtained. Experiments of this type are described in detail in Refs. 8 and 9. In Fig. 1 we plot the peak photocurrent at 80 K of sample I as a function of the applied voltage. The peak photocurrent exhibits a strong maximum at -3.6 V (the minus sign referring to the reverse direction) and a weaker maximum around -11 V. Both maxima can be explained by resonant coupling of adjacent wells in the superlattice. The first (second) maximum occurs at an applied voltage where the first and second (third) electronic subbands are aligned. Taking into account the built-in voltage of 1.5 V we esti-

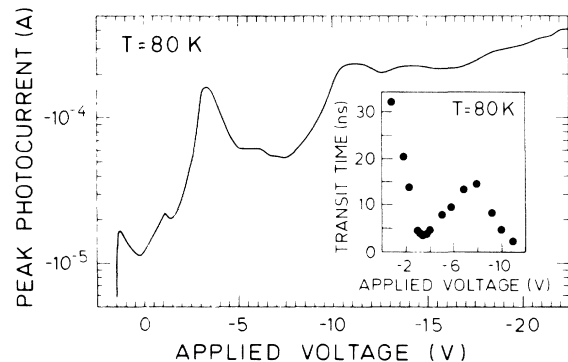


FIG. 1. Peak photocurrent vs applied voltage for sample I under 530-nm illumination. Inset: The transit time vs the applied voltage for the same sample.

mate from the positions of the maxima a subband spacing of 100 meV (250 meV). Photocurrent spectroscopy^{9,10} (PCS) gives a subband spacing of 86 meV (198 meV) at low electric fields. The difference between the values obtained by PCS and transport experiments arises from a partial depletion of the doped contact regions near the superlattice.

We conclude that the transport in this system is enhanced at certain applied voltages due to SRT, i.e., injection of electrons from the lowest subband into a higher subband of the adjacent well followed by rapid relaxation to the lowest subband. The inset of Fig. 1 shows the transit times through the whole intrinsic layer of sample I determined from the photocurrent transients. The transit time exhibits a minimum at the same applied voltage where the peak photocurrent has a pronounced maximum. The transit time at -3.6 V is 3 ns, which corresponds to a transport time of 60 ps per superlattice period. This transport time is a measure for the time it takes a carrier to reach the adjacent well. It should not be confused with the time constant for coherent resonant tunneling as discussed in Ref. 11.

Time-resolved PL experiments are performed with a synchronously pumped, mode-locked dye laser with a repetition rate of 80 MHz and a pulse width of 5 ps. The excitation wavelength can be varied between 650 and 790 nm by using two dyes (Pyridin-2 and DCM). The intensity of the excitation is adjusted between 1 and 2 mW to give an average photocurrent of the order of 200 μ A. The diameter of the focal spot is about 25 μ m resulting in a carrier density of the less than 10^{15} cm^{-3} . The luminescence is focused onto the entrance slit of a 0.32-m monochromator. A 2D streak camera is used to record the PL intensity as a function of time and energy. The overall time resolution of the system depends on the temporal dispersion of the monochromator and varies between 10 and 20 ps (full width at half maximum of the laser pulse on the streak camera).

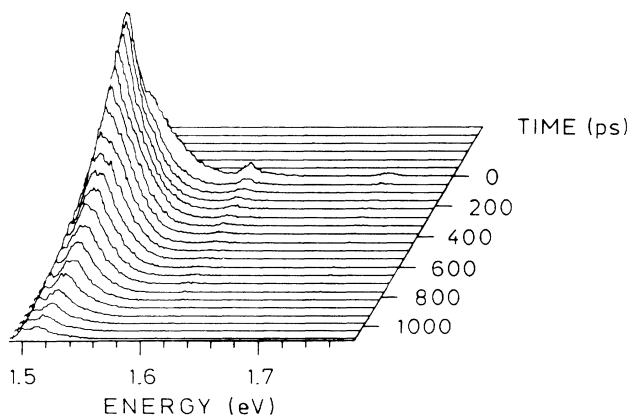


FIG. 2. Typical time-resolved photoluminescence spectrum for sample I at an applied voltage of -13 V and a temperature of 77 K.

A typical time-dependent PL spectrum of sample I at an applied voltage of -13 V and 77 K is shown in Fig. 2. The excitation wavelength is 652 nm (1.902 eV), i.e., carriers are excited above the third electronic subband. Three distinct features are observed. The strongest peak at 1.510 eV is due to the transition from the lowest conduction subband to the highest heavy-hole state (transition hh11). The energy is redshifted from its value at zero field due to the quantum-confined Stark effect.¹² A discussion of the detailed structure of this PL line is beyond the scope of this paper. A weaker peak is observed at 1.598 eV and assigned to the transition from the second electronic subband to the heavy-hole ground state (transition hh21). This identification can be made unambiguously by comparing this spectrum to the photocurrent spectrum at the same temperature and same applied electric field. A very weak peak is seen at 1.715 eV. It corresponds to the transition from the third electronic subband to the heavy-hole ground state (transition hh31). The time dependence is in most cases not purely exponential. It is therefore difficult to extract time constants from the transients.

The intensities of the second and third electronic subbands in the PL spectrum are strongly voltage dependent. In Fig. 3 we plot the PL spectrum of sample I at 200 ps after 652-nm excitation for different applied voltages. At -2 V there is no indication of the second- or third-subband PL present. At -5 V the second subband has clearly emerged, while the third subband is still not visible. At -10 V the intensity of the second subband has grown in strength relative to the PL intensity from

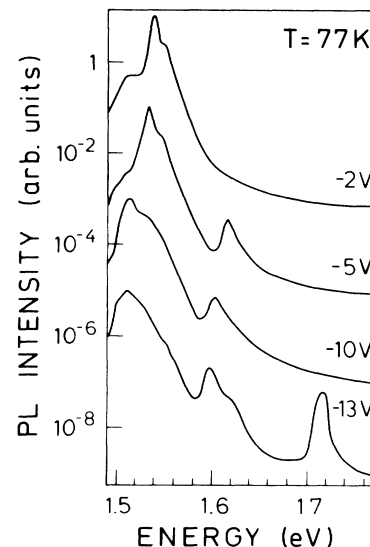


FIG. 3. Photoluminescence spectra of sample I at 200 ps after photoexcitation for different applied voltages. The different curves are shifted with respect to each other and have been smoothed for clarity. The high-energy background tail is due to the limited dynamical range of the streak camera.

the first subband. The third subband, on the other hand, does not appear below -11 V and is clearly observed at -13 V. The high-energy side of the PL from the lowest conduction subband decreases nearly exponentially with energy, revealing a carrier temperature of 80 – 90 K, which indicates a thermal population of the lowest conduction subband on this time scale. In sample II we also observe PL from the second subband between -3 and -6 V. The maximum value of the relative intensity of the second-subband PL is larger than in sample I. Because of the thinner barriers in sample II the transit time at higher fields becomes much shorter than the luminescence lifetime so that a significant PL signal of the second subband cannot be detected beyond -6 V.

When the excitation wavelength is changed to an energy between the first and second subbands (790 nm), we again observe PL from the second and third subbands with a similar voltage dependence. This is additional evidence that the population of the higher subbands is produced by SRT. The time dependence of the higher-subband PL displays a significant change at short times (< 100 ps) for excitation below the second subband. In this case, the PL signal rises within the time resolution to a maximum value and stays approximately constant out to about 100 ps. For excitation above the second subband the PL signal again rises to a maximum within the time resolution, but begins to decay immediately afterwards.

An interesting feature of the voltage dependence of the PL intensity is the fact that the hh21 luminescence does not disappear for applied voltages above the resonance condition. To get a better understanding of this feature we plot in Fig. 4 the intensity ratio of the hh21 and the hh11 transitions at 200 ps after excitation as a function of the applied voltage. Two regions of large in-

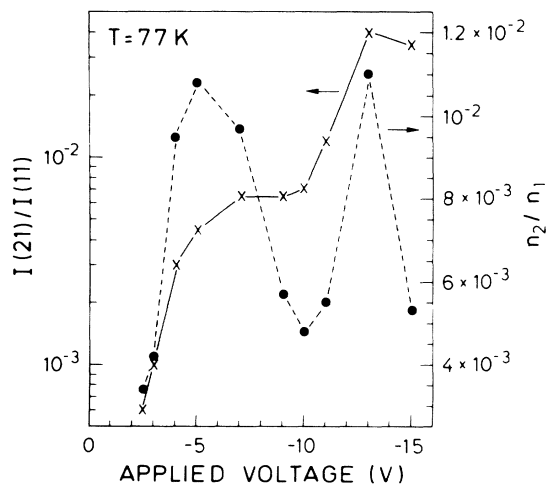


FIG. 4. Photoluminescence intensity ratio $I(21)/I(11)$ (solid line) for the hh21 and hh11 transitions and occupation ratio n_2/n_1 (dashed line) of the second and first subbands in sample I vs applied voltage. The lines are guides to the eye.

crease at both ends of the voltage scale are separated by a plateaulike region between -7 and -10 V. To extract the level of occupation from the measured PL intensities we have to take into account that the oscillator strengths of both transitions are strongly field dependent.^{13,14} The correct relation between occupations and intensities is

$$\frac{n_2}{n_1} = \frac{f_1 I_2}{f_2 I_1}, \quad (1)$$

when n_1 and n_2 are the occupations, f_1 and f_2 are the oscillator strengths, and I_1 and I_2 are the intensities of the hh11 and hh21 transitions, respectively. To determine the oscillator strength we take the peak height of the respective transitions from the photocurrent spectra¹⁴ that were measured at the same applied voltages and temperature. The resulting occupation ratio is also shown in Fig. 4. The largest occupations of the second subband are achieved at about -5 and -13 V close to the first and second resonances in the peak photocurrent of Fig. 1, which clearly supports the SRT picture. The maximum occupation ratio at -5 V is about 1.1×10^{-2} in this sample. In sample II the maximum occupation ratio is 6×10^{-2} . We conclude from the correlation between the voltage dependence of the occupation ratio and of the peak photocurrent that the occupation of the higher subbands is nonthermal.

To extract the intersubband relaxation time from the observed occupation ratios we can, in good approximation, neglect the effect of the recombination times and the transit time through the whole superlattice. The dynamics of the system is then determined by the intersubband relaxation time τ_1 and a transport time τ_2 which is a measure for the transport from one well to the adjacent well. Tunneling out of the higher subbands into the adjacent well or continuum can be neglected in this system due to the large barrier height of AIs. The time evolution of the population of the first and second subbands in the i th well can be described by

$$\frac{dn_1^i}{dt} = -\frac{n_1^i}{\tau_2} + \frac{n_2^i}{\tau_i} + G\delta(t) \quad (2)$$

and

$$\frac{dn_2^i}{dt} = -\frac{n_2^i}{\tau_1} + \frac{n_1^{i-1}}{\tau_2}. \quad (3)$$

n_1^i and n_2^i are the occupation of the first and second subbands in the i th well and G is the generation rate of the photoexcitation. We have assumed that carriers are only generated in the first subband, i.e., optical excitation below the second subband. To further simplify the analysis we set $n_1^{i-1} = n_1^i$, i.e., the number of carriers that enter the i th well by tunneling into the second subband is equal to the number that leave the same well by tunneling from the first subband. The solution of Eqs. (2) and (3) leads to a constant occupation ratio at long times

which is given by

$$\frac{n_2^i}{n_1^i} = \frac{\tau_1}{\tau_2}. \quad (4)$$

This result clearly shows that a finite occupation of the second subband can be achieved for transport times τ_2 , which are much shorter than the luminescence lifetime and transit time through the whole superlattice, but of the same order of magnitude as the intersubband relaxation time τ_1 . Equation (4) also holds for excitation into or above the second subband. In this case the time dependence at short times changes (in a similar way as observed in the experiments), but the behavior at very long times remains unchanged. We note that this result remains valid even when the luminescence lifetimes of both subbands are included in Eqs. (2) and (3), provided that τ_1 and τ_2 are much smaller than the PL lifetimes. A quasi-steady-state is reached for times longer than τ_1 and τ_2 and shorter than the PL lifetimes and the transit time.

In order to use Eq. (4) to estimate the intersubband relaxation time from the experimentally determined occupation ratios, we note that $n_{1,2} = \sum n_{1,2}^i$, where we sum over all the wells in the illuminated region. It can be shown for our systems that the occupation ratio in Eq. (4) is approximately equal to the experimentally observed occupation ratio in Eq. (1). Assuming a transport time $\tau_T = \tau_1 + \tau_2$ of 60 ps for sample I (as discussed above), the observed maximum occupation ratio yields an intersubband relaxation time of 0.65 ps, in good agreement with recent experimental⁵ and theoretical values.⁷ For sample II we assume the same oscillator strength. The transport time τ_T of 10 ps for sample II is taken from Ref. 15. The resulting intersubband relaxation time of 0.57 ps is in excellent agreement with the value obtained in sample I. We emphasize that the present method to determine the intersubband relaxation time does not require subpicosecond time resolution.

In summary, we have shown that a finite occupation of higher subbands in a GaAs-AlAs superlattice can be directly observed by photoluminescence spectroscopy, even for subband spacings larger than the optical-phonon energy. The voltage dependence of the relative occupation of the second subband is similar to the voltage dependence of the peak photocurrent, indicating a non-thermal population in the second subband. The mechanism for the occupation is sequential resonant tunneling. This is a resonantly enhanced transport process between two aligned energy levels with subsequent intersubband

relaxation. The relative occupation of the second subband together with the electrically measured transport time between adjacent wells was used to determine the intersubband relaxation time in a superlattice to be 0.6 ps, which is the same value as measured in independent quantum wells.

We would like to thank M. Hauser for sample growth, I. Jungbauer, F. Schartner, S. Tippmann, and M. Wurster for diode processing, and M. G. W. Alexander for a critical reading of the manuscript. This work was supported in part by the Bundesministerium für Forschung und Technologie.

^(a)Present address: Fraunhofer-Institut für Angewandte Festkörperphysik, Eckerstrasse 4, D-7800 Freiburg, Federal Republic of Germany.

¹M. Helm, P. England, E. Colas, F. DeRosa, and S. J. Allen, Jr., *Phys. Rev. Lett.* **63**, 74 (1989).

²D. Y. Oberli, D. R. Wake, M. V. Klein, J. Klem, T. Henderson, and H. Morkoc, *Phys. Rev. Lett.* **59**, 696 (1987).

³A. Seilmeier, H.-J. Hübner, G. Abstreiter, G. Weimann, and W. Schlapp, *Phys. Rev. Lett.* **59**, 1345 (1987).

⁴R. J. Bäuerle, T. Elsaesser, W. Kaiser, H. Lobentanzer, W. Stolz, and K. Ploog, *Phys. Rev. B* **38**, 4307 (1988).

⁵M. C. Tatham, J. F. Ryan, and C. T. Foxon, *Phys. Rev. Lett.* **63**, 1637 (1989).

⁶B. K. Ridley, *Phys. Rev. B* **39**, 5282 (1989).

⁷J. K. Jain and S. Das Sarma, *Phys. Rev. Lett.* **62**, 2305 (1989).

⁸H. Schneider, K. von Klitzing, and K. Ploog, *Europhys. Lett.* **8**, 575 (1989).

⁹H. Schneider, K. von Klitzing, and K. Ploog, *Superlattices Microstruct.* **5**, 383 (1989).

¹⁰R. Tsu, L. L. Chang, G. A. Sai-Halasz, and L. Esaki, *Phys. Rev. Lett.* **34**, 1509 (1975); R. T. Collins, K. von Klitzing, and K. Ploog, *Phys. Rev. B* **33**, 4378 (1986).

¹¹D. Y. Oberli, J. Shah, T. C. Damen, C. W. Tu, T. Y. Chang, D. A. B. Miller, J. E. Henry, R. F. Knopf, N. Sauer, and A. E. DiGiovanni, *Phys. Rev. B* **40**, 3028 (1989).

¹²D. A. B. Miller, D. S. Chemla, T. C. Damen, A. C. Gosard, W. Wiegmann, T. H. Wood, and C. A. Burrus, *Phys. Rev. Lett.* **53**, 2173 (1984).

¹³M. Matsuura and T. Kamizato, *Phys. Rev. B* **33**, 8385 (1986).

¹⁴P. W. Yu, G. D. Sanders, D. C. Reynolds, K. K. Bajaj, C. W. Litton, J. Klem, D. Huang, and H. Morkoc, *Phys. Rev. B* **35**, 9250 (1987); P. W. Yu, G. D. Sanders, K. R. Evans, D. C. Reynolds, K. K. Bajaj, C. E. Stutz, and R. L. Jones, *Phys. Rev. B* **40**, 3151 (1989).

¹⁵H. Schneider, W. W. Rühle, K. von Klitzing, and K. Ploog, *Appl. Phys. Lett.* **54**, 2656 (1989).